



## Straining of colloidal particles in saturated porous media

Shangping Xu,<sup>1</sup> Bin Gao,<sup>1</sup> and James E. Saiers<sup>1</sup>

Received 6 February 2006; revised 6 October 2006; accepted 26 October 2006; published 7 December 2006.

[1] Straining may influence the mobility of colloid-sized particles within groundwater aquifers as well as within granular filters that are used in wastewater treatment. We conducted column transport experiments using latex microspheres as the colloids and quartz sand as the porous medium to investigate the response of colloid straining to changes in colloid diameter ( $d_p$ ) and sand grain diameter ( $d_g$ ). For these experiments the negatively charged microspheres were suspended in deionized water, and the quartz sand was thoroughly cleaned to minimize physicochemical deposition (attachment), which permitted the determination of straining in an unambiguous way. The measurements of strained (immobile phase) and effluent (aqueous phase) colloid concentrations could be described with a transport model that accounted for an exponential decline in straining rates with increasing concentrations of strained colloids. Best fit values of the model coefficient that quantified clean bed straining rates ( $k_o$ ) were negligibly small for  $d_p/d_g < 0.008$  and, above this threshold, varied linearly with  $d_p/d_g$ . Our findings suggest that accurate inferences on the mobility of colloid-sized particles will require consideration of the effects of straining when  $d_p/d_g$  exceeds 0.008.

**Citation:** Xu, S., B. Gao, and J. E. Saiers (2006), Straining of colloidal particles in saturated porous media, *Water Resour. Res.*, 42, W12S16, doi:10.1029/2006WR004948.

### 1. Introduction

[2] Water quality issues associated with colloid-facilitated contaminant transport, groundwater pollution by microbial pathogens, wastewater treatment by packed bed filters, and bioremediation of contaminated groundwater aquifers drive efforts aimed at improving current understanding of the filtration of colloid-sized particles in porous media. A theory for physicochemical filtration of colloids within water-saturated porous media was advanced more than three decades ago [Yao *et al.*, 1971], and refinements of this theory have led to a framework appropriate for predicting the transport of colloids in model systems under some conditions [Rajagopalan and Tien, 1976; Tufenkji and Elimelech, 2004a]. This theory is derived from mathematical descriptions of water flow and colloid transport around a single collector (e.g., sand grain) and expresses a dimensionless colloid filtration rate as the product of the single-collector contact efficiency, which describes the rate at which pore fluid colloids strike the collector, and the sticking efficiency, which describes the probability that a colloid-collector collision will succeed in attachment [Elimelech, 1994]. Although physicochemical filtration theory does account for the effects of neighboring collectors on the flow field [Happel, 1958], it does not account for colloid immobilization by straining, retention that occurs when a colloid samples a constriction between adjacent mineral grains that is too narrow to permit passage. Several researchers have suggested that this failure to account for straining may be partially responsible for deviations

between measured colloid retention rates and those predicted by physicochemical filtration theory [Bradford and Bettahar, 2005; Bradford *et al.*, 2004, 2005, 2003, 2002; Li *et al.*, 2004; Tufenkji *et al.*, 2004].

[3] Straining has long been recognized as a mechanism of colloid retention, but has received less attention than physicochemical deposition (i.e., retention described by filtration theory that occurs when a colloid attaches to a collector). Herzig *et al.* [1970] computed criteria for colloid straining by model porous media composed of smooth and spherical collectors of uniform size and reported that triangular-shaped constrictions between three tangent collectors strain colloids when the ratio of colloid diameter to collector diameter ( $d_p/d_g$ ) exceeds 0.154 and that crevice sites between two tangent collectors contribute significantly to straining when  $d_p/d_g$  exceeds 0.05. Laboratory data on the transport of microspheres, bacteria and *Cryptosporidium* through packed beds suggest that the theoretical criteria of Herzig *et al.* [1970] underestimate the effects of straining on colloid retention and that straining is detectable at  $d_p/d_g$  as low as 0.002 [Bradford *et al.*, 2003, 2002; Foppen *et al.*, 2005; Li *et al.*, 2004].

[4] Breakthrough curve data measured in column experiments on microsphere and bacteria transport have been used to test mathematical models that solve the advection-dispersion equation together with kinetics equations for straining and deposition [Bradford and Bettahar, 2005; Bradford *et al.*, 2003; Foppen *et al.*, 2005]. The results of the model evaluations have proven critical in identifying appropriate forms of the kinetics expressions for straining; however, with no theoretical means to specify the kinetics parameters and with few published empirical relationships on straining kinetics [Bradford *et al.*, 2003], the response of straining rates to changes in the physical properties of the colloids and porous media remains poorly understood.

<sup>1</sup>School of Forestry and Environmental Studies, Yale University, New Haven, Connecticut, USA.

[5] The objective of this work is to quantify the effects of colloid and collector size on straining rates through analysis of results from experiments on the transport of latex microspheres through water-saturated columns and transparent flow cells packed with sand. We conducted experiments with  $d_p/d_g$  values ranging from 0.002 to 0.055, thereby substantially extending the published range, and designed experiments to minimize the potentially confounding effects of physicochemical deposition (colloid attachment to grain surfaces) so that straining rates could be determined in an unambiguous way. Our results indicate that straining influences colloid retention over a broad range of  $d_p/d_g$ , but that colloids may be less susceptible to straining than suggested by published experimental studies.

## 2. Experimental Methods

[6] Green latex microspheres (Magsphere Inc.) with carboxyl surface functional groups and diameters of 0.5  $\mu\text{m}$ , 1.1  $\mu\text{m}$ , 3.1  $\mu\text{m}$  and 5.1  $\mu\text{m}$  were used as the colloids in the column and flow cell experiments. Upon receipt from the manufacturer, the colloids were collected on Durapore membrane filters (Millipore) and redispersed in boiled deionized water eight times to remove surfactants from the colloid surfaces. Redispersion of the latex particles was facilitated by placing the suspension in an ultrasonic bath. The microspheres were negatively charged under our experimental conditions, and measurements of electrophoretic mobility (Brookhaven Instruments, ZetaPALs) equaled  $2.5 \times 10^{-8}$ ,  $3.6 \times 10^{-8}$ ,  $2.6 \times 10^{-8}$ , and  $2.1 \times 10^{-8} \text{ m}^2 \text{ s}^{-1} \text{ V}^{-1}$  for the 0.5, 1.1, 3.1, and 5.1  $\mu\text{m}$  microspheres, respectively.

[7] High-purity quartz sand (US Silica, Ottawa, IL and Unimin, New Canaan, CT) was used as the porous media in the column and flow cell experiments. Stainless steel sieves (VWR) were used to separate the sand into five size classes: 0.71–0.85 mm (denoted as 0.78 mm), 0.3–0.355 mm (0.33 mm), 0.125–0.15 mm (0.14 mm), 0.106–0.125 mm (0.12 mm), and 0.09–0.106 mm (0.098 mm). Impurities, such as iron hydroxide and organic coatings, and very fine particles were removed from the sand grain surfaces through a sequence of acid, base, and deionized water washes. The sieved sand was boiled for 24 hours in concentrated nitric acid (70%), rinsed with deionized water, washed for 12 hours on a shaker table with 0.1 M NaOH, and rinsed again with deionized water. Following this treatment, the coarsest sand (0.78 mm) was boiled a second time in concentrated nitric acid for 24 hours and thoroughly rinsed with deionized water. This nitric acid wash and deionized water rinse was repeated three times with the other sand size fractions, which, owing to their greater specific surface areas, had greater amounts of surface impurities than the coarsest sand. After the cleaning steps, the sand was dried in an oven at 80°C, and stored in covered Pyrex beakers until used in the experiments.

[8] Glass chromatography columns (Kontes<sup>®</sup>) equipped with Teflon end fittings and measuring 2.5 cm in diameter and 15 cm in length were used to contain the sand during the column experiments. Stainless steel membranes (with either 0.106 or 0.051 mm openings, Spectra/Mesh, Spectrum Laboratories, Inc.) emplaced inside the end fittings prevented movement of the sand, but allowed for the transmission of water and colloids. The columns were

oriented vertically and packed by slowly pouring the sand into deionized water standing at the bottom of the column. Layering due to differences in sand grain settling rates was minimized by maintaining the water level 0.5 to 1 cm above the sand surface during column packing. The porosity of the 0.78 and 0.33 mm sands equaled 0.36, and the porosity of the 0.14, 0.12, and 0.098 mm sands equaled 0.37.

[9] All column experiments were conducted in duplicate. Peristaltic pumps were used to deliver 40 pore volumes of deionized water to the tops of the column in order to equilibrate the sand pack prior to colloid injection. Measurements of influent and effluent pH taken near the end of this equilibration were approximately the same, ranging from 5.6 to 5.8. The specific discharge during the equilibration period was set  $0.31 \text{ cm min}^{-1}$ , which is greater than that encountered under natural gradient conditions in groundwater aquifers, the same order of magnitude as that encountered in riverbank filtration, and at the lower end of the flow rates associated with engineered, water treatment systems [Harvey *et al.*, 1993; Havelaar *et al.*, 1995].

[10] An experiment was initiated immediately after sand pack equilibration by introducing colloids to the top of the column. The colloids were suspended in deionized water (in order to enhance electrostatic repulsion between the colloids and sand grains and minimize deposition) at concentrations of  $1.45 \times 10^9$ ,  $1.36 \times 10^8$ ,  $6.08 \times 10^6$ ,  $4.09 \times 10^6$  particles  $\text{mL}^{-1}$  for the 0.5  $\mu\text{m}$ , 1.1  $\mu\text{m}$ , 3.1  $\mu\text{m}$ , and 5.1  $\mu\text{m}$  colloids, respectively. The colloids were applied for two hours (6.6 pore volumes), whereupon the column was flushed with colloid-free water at the same specific discharge ( $0.31 \text{ cm min}^{-1}$ ) until concentrations in the column effluent returned to baseline levels. Effluent samples were collected at selected intervals by a fraction collector and analyzed for colloid concentrations with a spectrophotometer (Beckman DU 520) at a wavelength of 650 nm.

[11] At the end of the four experiments on the transport of 3.1  $\mu\text{m}$  and 5.1  $\mu\text{m}$  colloids through the 0.098 mm and 0.012 mm sands, we disassembled the columns and measured the concentration of strained colloids as a function of depth within the sand pack. The sand was excavated under saturated conditions from top to bottom with a spatula in 1.5 cm increments and each increment was placed with 10 mL of deionized water into a 20 mL vial. After vigorously shaking the vial by hand for 10 seconds, 5 mL of supernatant was withdrawn and the concentration of colloids was measured at a wavelength of 650 nm with a spectrophotometer. The sand samples were dried at 80°C before measuring the weight of the sand in each 1.5-cm increment, and concentrations of strained colloids were expressed as the mass of colloids per unit mass of dry sand. Blank experiments conducted with clean sand (but with no colloids) showed that background turbidity from sand-derived particles was negligible.

[12] Column experiments with bromide, a conservative tracer, were conducted in the same way as the colloid transport experiments. Bromide concentrations in the effluent samples were measured with an ion chromatograph (Dionex DX500) equipped with an AS14 column, an anion suppressor, and a conductivity detector.

[13] Pore-scale visualization experiments have proven to be valuable in elucidating colloid retention and mobilization mechanisms in porous media [Gao *et al.*, 2006; Keller and

*Sirivithayapakorn*, 2004; *Sirivithayapakorn and Keller*, 2003a, 2003b]. In this research, a custom-built flow cell was used to make qualitative, pore-scale observations of colloid retention within the 0.098 mm sand. The flow cell was fabricated from transparent acrylic sheets and measured 6 cm in length, 1.6 cm in width, and 0.3 cm in depth. Two stainless steel membranes with 51  $\mu\text{m}$  pores were sealed between rubber gaskets at the inlet and outlet ends of the flow cell. The flow cell was wet packed with 5 g of sand, placed horizontally on the stage of an inverted visible light microscope (Nikon Eclipse TE2000-U), and connected to a syringe pump with Teflon tubing.

[14] The visualization experiments were initiated by applying a suspension of 5.1  $\mu\text{m}$  colloids to the inlet end of the flow cell at a specific discharge of 0.23  $\text{cm min}^{-1}$ . Following a 1-hour (6.2 pore volumes) injection of the colloid suspension, the flow cell was flushed with colloid-free deionized water for two hours (12.4 pore volumes) without perturbing the flow rate. At this stage, the flow cell was sealed at both ends after being disconnected from the syringe pump and pore-scale images were recorded at a magnification of 200X with a three-channel charge-coupled device camera (DAGE-MTI, DC330). A frame grabber card (Compix Inc.) with manufacturer-supplied software was used to acquire and process images.

### 3. Mathematical Model

[15] In order to quantify the kinetics of straining in our column experiments, we compared measured breakthrough curves to those calculated by a phenomenological model for colloid transport and straining. The model presented here is derived under the assumptions that straining rates vary with changes in the suspended and strained colloid concentrations and that straining is irreversible and represents the sole mechanism of retention. We also assume, in accordance with the pore-scale observations of *Li et al.* [2006a], that colloids are strained within pore space constrictions that occur around the contacts of adjacent mineral grains and that strained colloids form aggregates near the grain-to-grain contacts with continued loading. Resistance to flow through these aggregates increases as they grow in size, which causes the fluid streamlines to gradually migrate from the aggregate interiors to aggregate perimeters [*Veerapaneni and Wiesner*, 1996]. This shift in the fluid streamlines leads to a decline in straining rates as the colloid-carrying fluid is diverted around the perimeters of the aggregates and toward the centers of the pores, where the dimensions of the void spaces are greater than those of the colloids. Colloids that are transmitted through this portion of the void space should not be susceptible to straining, nor should they be influenced significantly by physicochemical deposition (at least in our experiments) because conditions and materials were chosen to maximize repulsive interaction forces between the colloids and sand grains.

[16] The advection-dispersion equation describes the transport of colloids:

$$\frac{\partial C}{\partial t} + \frac{\rho_b}{n} \frac{\partial S}{\partial t} = -v \frac{\partial C}{\partial x} + D \frac{\partial^2 C}{\partial x^2} \quad (1)$$

where  $C$  is the concentration of colloids suspended in the pore water,  $t$  is time,  $\rho_b$  is the bulk density,  $n$  is porosity,  $S$  is

the concentration of strained colloids (mg colloid/g sand),  $v$  is the average linear pore water velocity,  $x$  is the coordinate parallel to flow, and  $D$  is the hydrodynamic dispersion coefficient. Our assumption that straining is restricted to the small portion of the void space near the grain-to-grain contacts implies that permeability reduction associated with colloid accumulation is small and hence the hydraulic head gradient and  $v$  in equation (1) can be approximated as constant.

[17] Equation (1) is coupled with a parametrically simple kinetics equation that is first order in  $C$  and describes an exponential decline in straining rates with increasing  $S$ , such that

$$\frac{\rho_b}{n} \frac{\partial S}{\partial t} = k_o C e^{-S/\lambda} \quad (2)$$

where  $k_o$  is a rate coefficient that quantifies straining kinetics under clean bed conditions, when  $S \approx 0$ , and  $\lambda$  is a coefficient with the same units as  $S$  that quantifies the exponential decline in straining rates from the maximum, clean bed rate of  $k_o C$  as  $S$  increases from its initial value of zero. According to equation (2), the straining rate equals  $0.37 k_o C$  when  $S = \lambda$ , declines to  $0.018 k_o C$  as  $S$  increases to  $4\lambda$ , and becomes vanishingly small with further increases in  $S$ . The parameter  $\lambda$ , then, is analogous (but not equal) to the straining capacity of the porous medium, in as much that this parameter determines the values of  $S$  in which straining rates become negligibly small such that colloid retention effectively ceases.

[18] Equations (1) and (2) are assumed to govern the coupled transport and straining of colloids within our sand columns. These equations were approximated by a second-order, finite difference scheme for semi-infinite column with a first-type boundary condition at the column inlet, and the resulting system of equations was solved iteratively to obtain concentrations of pore water and strained colloids as a function of time and depth within the column.

[19] We quantified the kinetics of colloid straining by fitting numerical solutions of equations (1) and (2) to the colloid breakthrough data. In these inverse simulations, a Levenberg-Marquadt least squares algorithm was used to find the best fit values of  $k_o$  and  $\lambda$  or, in other words, the values of  $k_o$  and  $\lambda$  that minimized the sum of the squared residuals between measured and model breakthrough concentrations [*Press*, 1989]. The value of  $v$  was calculated from measurements of sand pack porosity and specific discharge, while values of  $D$  were determined by fitting solutions of equation (1) (for the case of  $\frac{\partial S}{\partial t} = 0$ ) to the bromide breakthrough data.

## 4. Results

### 4.1. Flow Cell Experiments

[20] Retention of the 5.1  $\mu\text{m}$  colloids was readily apparent within the flow cell experiments (Figure 1). Colloids accumulated in the highest concentrations where the pore spaces narrowed near the contacts of irregularly shaped sand grains, indicating that these pore space constrictions served as favorable locations for colloid retention by straining. Comparatively few colloids were immobilized in areas toward the centers of the sand grains, away from the grain-



**Figure 1.** Pore-scale image of the accumulation of  $5.1 \mu\text{m}$  colloids retained near the grain-to-grain contact of the  $0.098 \text{ mm}$  sand. The aggregate of strained colloids that formed around the grain-to-grain contact is circled. Color appears in back of the print issue.

to-grain contacts, which suggests that strong repulsive forces between the colloids and the thoroughly cleaned sand limited physicochemical deposition.

#### 4.2. Column Experiments

[21] The breakthrough curves of bromide exhibited little sensitivity to changes in grain size (Figure 2) and closely resembled the breakthrough curves measured in the seven colloid transport experiments in which the ratio of colloid diameter ( $d_p$ ) to grain diameter ( $d_g$ ) was less than 0.005 (Figures 3a–3c and Table 1). Steady state effluent concentrations exceeded 0.99 in the experiments conducted with the  $0.5 \mu\text{m}$  colloids and the  $0.78 \text{ mm}$ ,  $0.33 \text{ mm}$ ,  $0.14 \text{ mm}$ , and  $0.12 \text{ mm}$  sands (Figure 3a). In a similar fashion, the transport of the  $1.1 \mu\text{m}$  colloids through the  $0.78 \text{ mm}$  and  $0.33 \text{ mm}$  sands and the transport of the  $3.1 \mu\text{m}$  colloids through the  $0.78 \text{ mm}$  was unaffected by retention processes as, for each of these treatments, greater than 99% of the injected colloid mass was recovered from the column effluent (Table 1).

[22] Colloid retention was clearly detectable in the 13 experiments in which  $d_p/d_g$  exceeded 0.005. Maximum breakthrough concentrations measured in the experiments with the  $0.5 \mu\text{m}$  colloids and  $0.098 \text{ mm}$  sand equaled 0.97 (Figure 3a) and were lower in the experiments with the  $1.1 \mu\text{m}$  colloids and the  $0.14 \text{ mm}$ ,  $0.12 \text{ mm}$ , and  $0.098 \text{ mm}$  sand (Figure 3b), where 5% to 7% of the applied colloids were retained within the sand packs (Table 1). Changes in grain size exerted a strong influence on the retention of the  $3.1 \mu\text{m}$  colloids (Figure 3c). As grain size decreased from  $0.78$  to  $0.098 \text{ mm}$ , maximum breakthrough concentrations of the  $3.1 \mu\text{m}$  colloids decreased from  $>0.99$  to  $0.72$ , while the percentage of colloids that were retained within the column increased from  $<1$  to 50%. Effluent concentrations in the experiments with the  $5.1 \mu\text{m}$  colloids exhibited the same slow increase toward steady state levels as those measured in the experiments with the  $3.1 \mu\text{m}$  colloids (Figure 3d); however, breakthrough concentrations were lower (and thus more colloids were immobilized) in

the experiments with the  $5.1 \mu\text{m}$  colloids. Colloid retention was greatest in the experiment with the  $5.1 \mu\text{m}$  colloids and  $0.098 \text{ mm}$  sand (Table 1). At the end of this experiment, the total volume of colloids retained equaled  $0.0484(\pm 0.00094) \text{ mL}$ , which corresponds to 0.18% of the total column void space. We do not expect that the permeability of the sand packs was reduced at these low colloid accumulations, although we did not make measurements of hydraulic head that could be used to confirm this assumption.

[23] The concentrations of colloids retained within the column at the end of the experiment exhibited little spatial variability between the top and bottom of the sand pack (Figure 4). Calculations based on the mass of colloids applied to the sand packs, mass of colloids recovered from the base of the columns, and the total mass of retained colloids indicated that our extraction method succeeded in recovering from 61 to 88% of the strained colloid fraction, depending on grain and colloid size (Table 1). For comparison with our modeled results (see below), we adopted a published approach [Bradford and Bettahar, 2006; Tufenkji and Elimelech, 2004b] and adjusted the measurements by dividing the strained colloid concentrations by the recovery efficiency (Table 1), and, in accordance with published studies [Bradford and Bettahar, 2006; Tufenkji and Elimelech, 2004b], we assumed that the recovery efficiency was constant within an experiment.

#### 4.3. Comparison of Experimental and Modeled Results

[24] Agreement between modeled and observed concentration is generally good with  $R^2$  values (a measure of the goodness of model fit) ranging from 0.93 to unity and exceeding 0.97 for 24 of the 26 simulations (Table 1). The most consistent deviation between measured and modeled concentrations occurs between 8 and 9 pore volumes, when the model underestimates the tailing concentrations. This discrepancy reveals that, counter to our simplifying assumption, colloid straining in our experiments was not completely irreversible. Nevertheless, the underestimation of eluted colloid mass does not exceed 7% and is generally less than

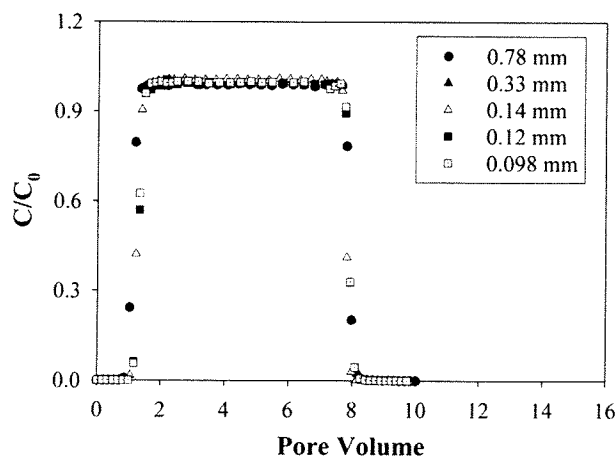


**Figure 2.** Measured breakthrough curves for bromide, a conservative tracer. Legends describe the size of sand grains.

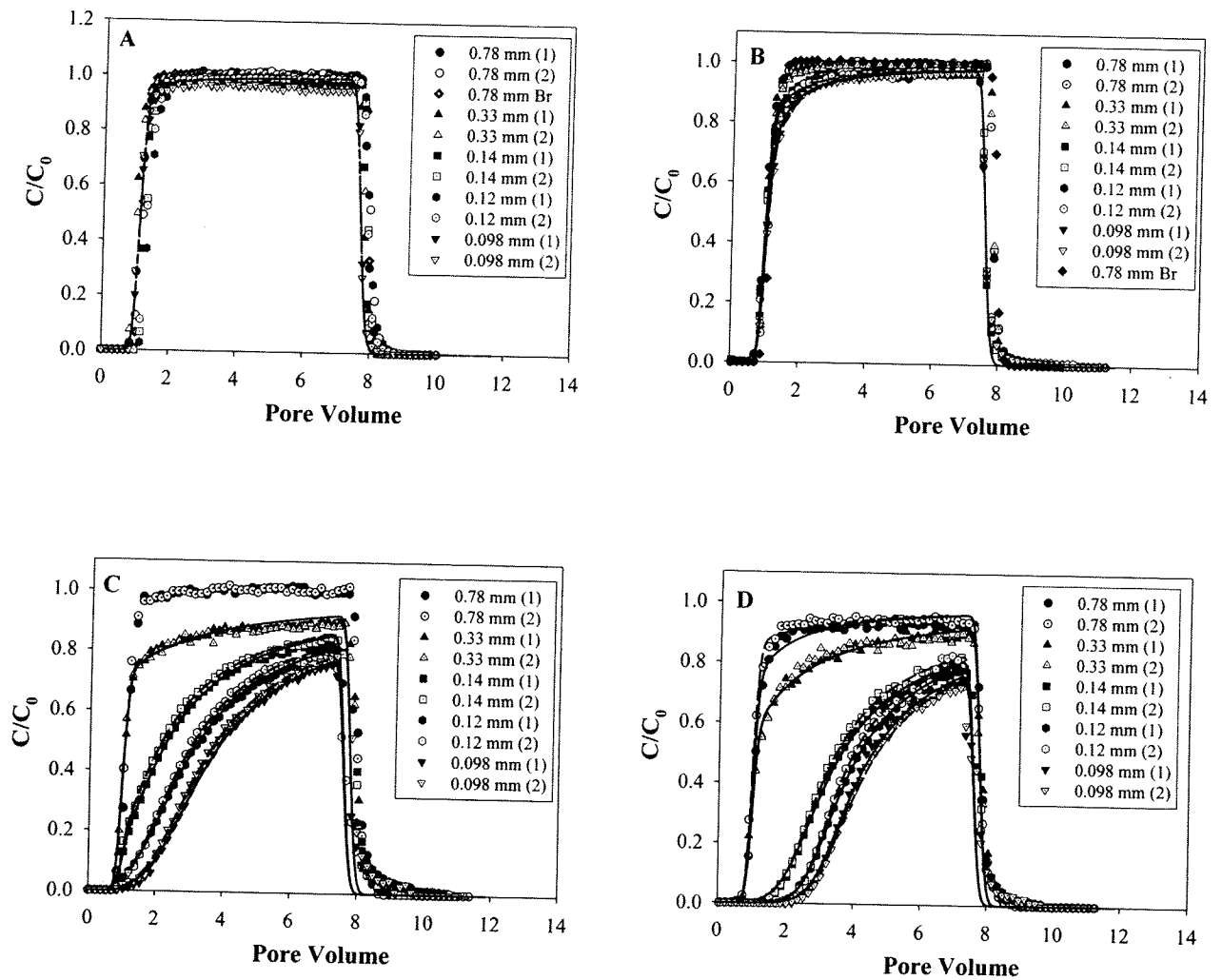


**Figure 3.** Breakthrough curves measured in duplicate experiments on the transport of (a) bromide and  $0.5 \mu\text{m}$  colloids, (b) bromide and  $1.1 \mu\text{m}$  colloids, (c)  $3.1 \mu\text{m}$  colloids, and (d)  $5.1 \mu\text{m}$  colloids. Symbols represent observed concentrations, and lines represent model-calculated breakthrough concentrations. Legends describe the size of sand grains.

5%, suggesting that application of a reversible rate law with additional adjustable parameters is unwarranted. The generally good agreement between measured and modeled breakthrough curves suggests that colloid dispersion could be quantified using values of the hydrodynamic dispersion coefficient ( $D$ ) estimated from inverse analysis of the bromide breakthrough curves. Because of the homogeneity of the sand packs and the small length scale for transport, estimates of  $D$  exhibited low sensitivity to changes in grain size, equaling 0.11, 0.091, 0.11, 0.13 and  $0.10 \text{ cm}^2 \text{ hour}^{-1}$  for the 0.78, 0.33, 0.14, 0.12 and 0.098 mm sands, respectively. Variation in  $D$  over the observed range (0.09 and  $0.13 \text{ cm}^2/\text{min}$ ) had only a minor effect on the appearance of the simulated breakthrough curves.

[25] The mathematical model was evaluated further by comparing its calculations of strained colloid concentrations with those measured at the end of the column experiments (Figure 4). Although the model fails to capture all the variability in these data, it does mimic the roughly uniform nature of the strained concentration

profiles. This reasonable approximation of the strained colloid concentrations, together with the close description of the breakthrough data, suggests that the form of equation (2) is appropriate for approximating straining in our column experiments.

#### 4.4. Best Fit Values of Model Parameters

[26] The best fit values of  $k_o$ , the rate coefficient for clean bed straining, range from zero to  $34.5 \text{ h}^{-1}$  (Table 1) and vary discernibly with the ratio of colloid diameter ( $d_p$ ) to sand grain diameter ( $d_g$ ). Estimates of  $k_o$  are generally zero and do not exceed  $0.9 \text{ h}^{-1}$  (average of duplicate experiments) below a threshold  $d_p/d_g$  value of 0.008 and vary linearly with  $d_p/d_g$  above this threshold value (Figure 5). The model parameter  $\lambda$  quantifies the relationship between retention rates and strained colloid concentrations. Values of  $\lambda$  increase with  $d_p$ , exhibit little variation with changes in  $d_g$  for experiments with the  $1.1 \mu\text{m}$  colloids, but increase monotonically with decreasing  $d_g$  for the experiments with the  $3.1 \mu\text{m}$  and  $5.1 \mu\text{m}$  colloids (Table 1). A

**Table 1.** Optimal Parameter Values Estimated From Column Breakthrough Curves<sup>a</sup>

Sand	$d_p/d_g$	Colloid, $\mu\text{m}$	$K_0$ , $\text{hour}^{-1}$	$\lambda$ , $\text{mg/g}$	$R^2$	Percent of Colloids Retained	Recovery Efficiency <sup>b</sup>
0.78 mm	0.00064	0.5	0	N. A.	N. A.	<1%	N. A.
0.78 mm	0.00064	0.5	0	N. A.	N. A.	<1%	N. A.
0.33 mm	0.0015	0.5	0	N. A.	N. A.	<1%	N. A.
0.33 mm	0.0015	0.5	0	N. A.	N. A.	<1%	N. A.
0.14 mm	0.0036	0.5	0	N. A.	N. A.	1%	N. A.
0.14 mm	0.0036	0.5	0	N. A.	N. A.	1%	N. A.
0.12 mm	0.0042	0.5	0	N. A.	N. A.	<1%	N. A.
0.12 mm	0.0042	0.5	0	N. A.	N. A.	<1%	N. A.
0.098 mm	0.0051	0.5	0.46	0.00075	1.00	4%	N. A.
0.098 mm	0.0051	0.5	0.26	0.00075	0.99	3%	N. A.
0.78 mm	0.0014	1.1	0	N. A.	N. A.	<1%	N. A.
0.78 mm	0.0014	1.1	0	N. A.	N. A.	1%	N. A.
0.33 mm	0.0033	1.1	0	N. A.	N. A.	<1%	N. A.
0.33 mm	0.0033	1.1	0	N. A.	N. A.	1%	N. A.
0.14 mm	0.0079	1.1	0.71	0.0030	1.00	5%	N. A.
0.14 mm	0.0079	1.1	1.1	0.0028	1.00	5%	N. A.
0.12 mm	0.0092	1.1	0.78	0.0032	1.00	5%	N. A.
0.12 mm	0.0092	1.1	0.98	0.0028	1.00	5%	N. A.
0.098 mm	0.011	1.1	1.9	0.0029	1.00	6%	N. A.
0.098 mm	0.011	1.1	2.2	0.0031	1.00	7%	N. A.
0.78 mm	0.0040	3.1	0	N. A.	N. A.	<1%	N. A.
0.78 mm	0.0040	3.1	0	N. A.	N. A.	<1%	N. A.
0.33 mm	0.0094	3.1	1.2	0.013	0.97	12%	N. A.
0.33 mm	0.0094	3.1	1.1	0.016	0.98	13%	N. A.
0.14 mm	0.022	3.1	6.5	0.019	0.97	32%	N. A.
0.14 mm	0.022	3.1	5.9	0.018	0.98	31%	N. A.
0.12 mm	0.026	3.1	11.6	0.023	0.93	42%	88%
0.12 mm	0.026	3.1	11.4	0.021	0.98	41%	84%
0.098 mm	0.032	3.1	16.2	0.025	0.97	50%	75%
0.098 mm	0.032	3.1	15.7	0.024	0.95	46%	61%
0.78 mm	0.0065	5.1	1.1	0.015	0.99	12%	N. A.
0.78 mm	0.0065	5.1	0.52	0.020	1.00	10%	N. A.
0.33 mm	0.015	5.1	2.0	0.038	0.99	16%	N. A.
0.33 mm	0.015	5.1	2.0	0.038	0.99	17%	N. A.
0.14 mm	0.036	5.1	19.3	0.063	0.97	45%	N. A.
0.14 mm	0.036	5.1	20.9	0.058	0.98	45%	N. A.
0.12 mm	0.043	5.1	31.4	0.065	0.98	54%	71%
0.12 mm	0.043	5.1	34.5	0.060	0.99	53%	71%
0.098 mm	0.052	5.1	33.8	0.071	0.97	59%	72%
0.098 mm	0.052	5.1	33.2	0.074	0.97	61%	66%

<sup>a</sup>N.A. is not applicable.

<sup>b</sup>Recovery efficiency equals ratio of the mass of colloids recovered in the extraction experiment to the total mass of colloids retained in the columns (determined from the area beneath the breakthrough curves).

linear equation (i.e.,  $\lambda = 1.44d_p/d_g - 0.004$ ) accounts for 81% of the variation in the relationship between  $\lambda$  and  $d_p/d_g$  (Figure 6).

## 5. Discussion

[27] Our interpretation of the data is based on the assumption that straining, rather than physicochemical deposition, dominated colloid retention in our experiments. This assumption is supported by calculations of the net interaction energy profiles, made by summation of equations for electrical double-layer and van der Waals interaction energies [Gregory, 1981; Hogg *et al.*, 1966] according to the theory of Derjaguin, Landau, Verwey, and Overbeek (DLVO). The net interaction energy barrier exceeds  $293 k_bT$  (where  $k_b$  is Boltzmann constant and  $T$  is absolute temperature) for all treatments tested, which is high enough to prevent deposition in the primary minimum. Furthermore, secondary minima are absent from the net interaction energy profiles. Several studies have shown that colloids can adhere to collectors with rough or chemically heterogeneous surfaces even when

DLVO-based calculations predict that this attachment should not occur [Bhattacharjee *et al.*, 1998; Shellenberger and Logan, 2002; Song *et al.*, 1994]; therefore the interaction energy calculations are not sufficient to definitively exclude physicochemical deposition as a retention mechanism. Nevertheless, our observations suggest that this physicochemical deposition induced by surface roughness or chemical heterogeneity was small. Images recorded during the visualization experiments with the 0.098 mm sand and  $5.1 \mu\text{m}$  colloids revealed that colloid immobilization occurred almost exclusively near the grain-to-grain contacts, suggesting that straining, not physicochemical deposition, governed retention. Colloid transport through the sand columns mimicked that of a conservative solute tracer in experiments in which  $d_p/d_g < 0.005$ , indicating that physicochemical deposition was negligible for these seven treatments, which used, in some combination, all but 0.098 mm sand and  $5.1 \mu\text{m}$  colloids. Given that the compositions of the colloids, porous medium, and pore water were the same for all column experiments reported in this study, we infer that physicochemical deposition was similarly negligible in the

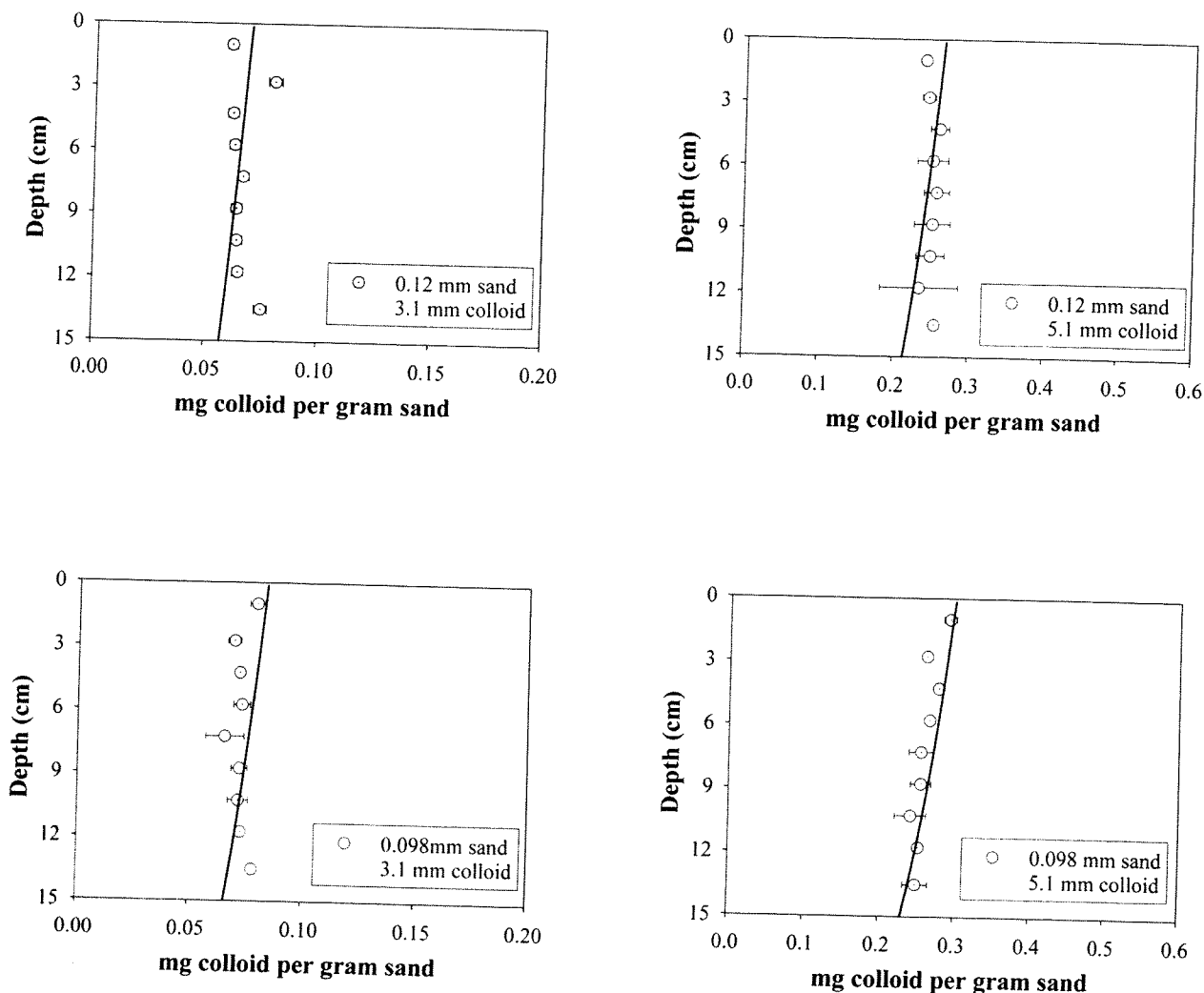


**Figure 4.** Measured (symbols) and model-predicted (lines) profiles of retained 3.1 and 5.1  $\mu\text{m}$  colloids in 0.12 mm and 0.098 mm sands. Strained-particle concentrations were obtained by dividing the measured concentrations by the recovery efficiencies listed in Table 1. The coefficient of variation (standard deviation of the measured values divided by the mean of the measured values) did not exceed 0.1 and was less than 0.06 for three of the four treatments.

13 column experiments in which  $d_p/d_g > 0.005$  and that the retention detected in these experiments can be attributed to straining.

[28] We find that clean bed straining rates, as quantified by  $k_o$ , are generally zero below a threshold  $d_p/d_g$  value 0.008 and increase linearly as  $d_p/d_g$  increases from 0.008 to 0.052 (Figure 5 and Table 1). Although straining contributed to the breakthrough response measured in 13 of our 20 experiments, our estimates of straining rates are considerably lower than published estimates [Bradford *et al.*, 2003]. Bradford *et al.* [2003] reported a threshold  $d_p/d_g$  value of 0.002, a factor of four less than our estimate, and reported that beyond this threshold clean bed straining rates varied exponentially with  $d_p/d_g$  according to  $269.7(d_p/d_g)^{1.42}$  [Bradford *et al.*, 2003, Figure 5]. For  $d_p/d_g = 0.021$ , the highest value tested by Bradford *et al.* [2002], the value of clean bed straining rate coefficient computed from their power law relationship is  $67.08 \text{ hour}^{-1}$ , which is seven times greater than the value determined from our linear relationship.

[29] We cannot definitively account for the variation between studies. The specific discharge in our experiments was nearly three times greater than that reported by Bradford *et al.* [2002], but we do not believe that this difference in flow rate is responsible for the disparity in the clean bed straining rates. We hypothesize that straining rates should decline with decreasing specific discharge as the flux of particles toward pore space constrictions (where straining occurs) decreases. According to this hypothesis, lowering the flow rates in our experimental system to match the specific discharge of Bradford *et al.* [2002] would reduce the clean bed straining rates and increase the gap between our estimates and those of Bradford *et al.* [2003].

[30] The sands used here and by Bradford *et al.* [2003] were collected from different sources and hence likely differed with respect to porous medium properties (other than  $d_g$ ) that may affect straining. Grain shape and roughness, for example, influence the length of the grain-to-grain contacts [Li *et al.*, 2006b] and grain size distribution affects

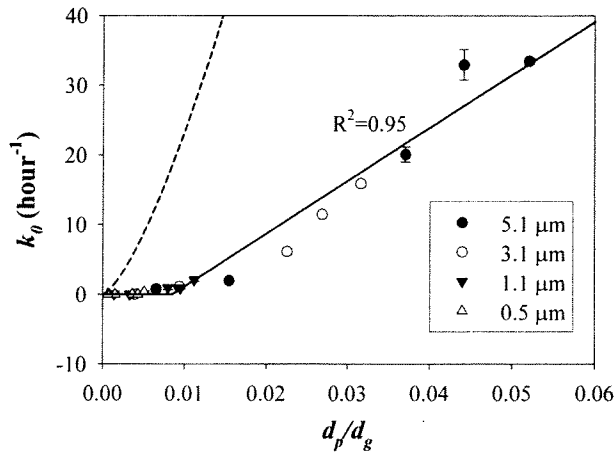


**Figure 5.** Empirical relationship between the clean bed straining rate coefficient,  $k_0$ , and the ratio of colloid diameter to sand grain diameter ( $d_p/d_g$ ). Error bars denote the standard deviation of duplicate experiments. The regression equation for the solid line is  $k_0 = 760 \frac{d_p}{d_g} - 6.4$ , for  $\frac{d_p}{d_g} > 0.008$ . The dashed line represents the empirical relationship presented by Bradford *et al.* [2003].

pore size. Tufenkji *et al.* [2004] reported that breakthrough concentrations of 4.1  $\mu\text{m}$  microspheres were greater in experiments with smooth, spherical glass beads than in experiments with irregularly shaped quartz sand, supporting the notion that grain shape influences straining. We did not measure grain shape, roughness, or grain size distribution, and published relationships between these textural features and straining rates are unavailable. Consequently, we are unable to test our hypothesis that differences in textural characteristics contribute, at least in part, to the disparity in clean-bed straining rates between Bradford *et al.* [2003] and those reported here.

[31] Another source of between-study variation could arise from differences in the way the sands were prepared and the experimental results were interpreted. We devoted considerable attention to cleaning the quartz sand in order to minimize physicochemical deposition (attachment) so that the straining rates could be determined unambiguously through inverse modeling. Both straining and physicochemical deposition affected colloid transport in the experiments of Bradford *et al.* [2002] and thus a portion of the deposition response (determined through model inversion) could have been attributed to straining, leading to an overestimation of clean bed straining rates.

[32] Our empirical estimates of  $k_0$  can be compared to published estimates of physicochemical deposition rates to evaluate, in a preliminary way, the relative contribution of straining to total colloid retention under conditions that favor colloid attachment. We do this by computing  $k_0/k_{dep}$ , where  $k_0$  is taken directly from our analysis and  $k_{dep}$ , the physicochemical deposition coefficient, is calculated for physical conditions that match those used in our column experiments, but for chemical conditions that favor colloid attachment. According to classical filtration theory [Yao *et al.*, 1971; Rajagopalan and Tien, 1976; Tufenkji and Elimelech, 2004a], the physicochemical deposition coefficient can be expressed as a function of the product of the

single-collector contact efficiency ( $\eta$ ) and the sticking efficiency ( $\alpha$ ):

$$k_{dep} = \frac{3(1-n)v}{2d_g} \alpha \eta \quad (3)$$

Values of  $\eta$  can be calculated for our experimental conditions with the correlation equations of Tufenkji and Elimelech [2004a]. Values of  $\alpha$  vary from zero to unity, with most published measurements ranging from 0.001 to 1. Measurements at the low end of this range were made with like-charged colloids and collectors at low ionic strengths [Abudalo *et al.*, 2005; Elimelech *et al.*, 2000; Kuznar and Elimelech, 2004; Redman *et al.*, 2004; Tufenkji and Elimelech, 2004b], while measurements near unity were often (but not always) made at high ionic strengths or with oppositely charged colloids and collectors [Elimelech *et al.*, 2000; Redman *et al.*, 2004]. Calculations of  $k_0/k_{dep}$  for the 0.5  $\mu\text{m}$  colloids are considerably less than unity for  $0.001 \leq \alpha \leq 1$ , indicating that straining plays a minor role in the retention of these submicrometer colloids, even when physicochemical deposition rates lie near the low end of expected values (Figure 7). Straining rates for colloids with diameters in excess of 1.1  $\mu\text{m}$  are generally equal to, and as much as 2.5 times greater than, physicochemical deposition rates for  $\alpha \sim 0.1$ . Under the most favorable conditions for attachment (i.e.,  $\alpha = 1$ ), physicochemical deposition is the major contributor to the immobilization of colloids with  $d_p > 1.1 \mu\text{m}$ , but, even in this case, straining rates are not negligible, equaling 10% to 25% of the deposition rates.

[33] The parameter  $\lambda$  in equation (2) is related to the effective straining capacity of the porous medium (see section 3) and governs the relationship between straining rates and the concentration of strained colloids ( $S$ ). Results of the inverse simulations reveal that best fit values of  $\lambda$  increase in an approximately linear fashion with  $d_p/d_g$ . This positive correlation reflects, in part, an increase in the number of locations for straining (grain-to-grain contacts) per mass of sand with decreasing  $d_g$  and,

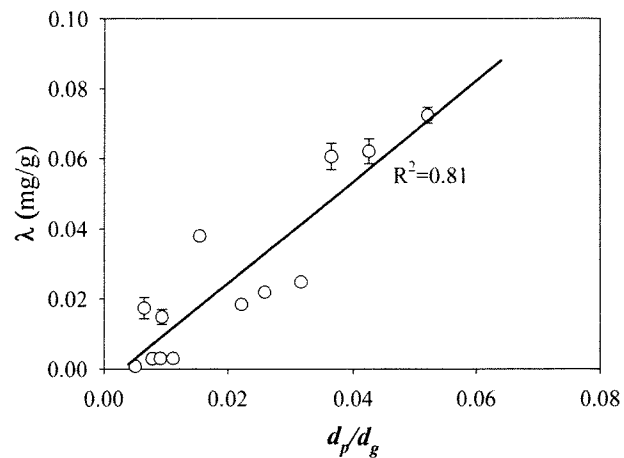


**Figure 6.** Relationship between best fit values of  $\lambda$  (see equation (2)) and  $d_p/d_g$ . Error bars denote the standard deviation of duplicate experiments. The regression equation for the solid line is  $\lambda = 1.44 \frac{d_p}{d_g} - 0.004$ .

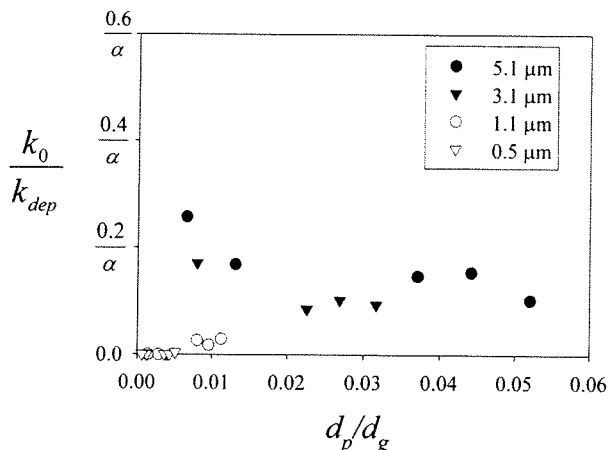


**Figure 7.** Comparison between the clean bed straining rate coefficient ( $k_0$ ) and colloid deposition rate coefficient ( $k_{dep}$ ) as a function of the ratio of the colloid diameter to sand grain diameter ( $d_p/d_g$ ). The values of  $k_0$  were averaged from duplicate experiments, while the values of  $k_{dep}$  were determined from equation (3) with values of  $\eta$  computed for our experimental conditions using the correlation equations presented by Tufenkji and Elimelech [2004a]. Notice that the y axis values are normalized by  $\alpha$ .

relatedly, an increase in the fraction of pore space with dimensions smaller than the colloids with increasing  $d_p/d_g$ . There is, however, scatter in the linear relationship between  $\lambda$  and  $d_p/d_g$ , suggesting that other factors, in addition to grain and colloid size, may influence the magnitude of  $\lambda$ . Similarly to the clean bed straining coefficient ( $k_0$ ),  $\lambda$  may be sensitive to mineral grain roughness and shape because these properties affect the geometry of the pore space. We also suspect that changes in pore water velocity could influence the magnitude of  $\lambda$  by affecting the morphology of the strained colloid aggregates. Veerapaneni and Wiesner [1997] conducted column experiments at specific discharges ranging from  $0.4 \text{ cm min}^{-1}$  to  $30.6 \text{ cm min}^{-1}$  and observed that compact, low-porosity colloidal aggregates formed within columns of quartz sand at high flow rates, while more porous colloidal deposits that occupied comparatively more pore space formed at low flow rates. These column experiments were conducted with sub-micrometer colloids under chemical conditions that favored physicochemical deposition (i.e., no interaction energy barrier), so the experimental results should not be interpreted as confirmation that the morphology of strained (as opposed to attached) colloids would exhibit the same flow rate dependence. Nevertheless, the observations of Veerapaneni and Wiesner [1997] suggest that changes in pore water velocity may influence the magnitude of  $\lambda$  by regulating the density and shape of the strained colloid aggregates.

[34] The strained concentrations of colloids measured after the termination of our column experiments exhibited rather small variation over the depth of the sand pack. In contrast, Bradford *et al.* [2002] reported that retained colloid concentrations were highest near the surface of the column and decreased monotonically with depth. The differences in the strained colloid profiles could be due, in part, to the contribution of physicochemical deposition to

colloid retention in the experiments of Bradford *et al.* [2002]. We believe, however, that differences in the mass of the colloids applied to the sand packs were primarily responsible for the dissimilarity in the strained colloid profiles. The colloid mass per column cross-sectional area applied to our sand columns was 13 to 22 times greater than that applied in the experiments of Bradford *et al.* [2002]. Because of the comparatively large colloid loadings in our experiments, the concentrations of strained colloid approached the effective straining capacity of the porous medium and thus the straining rates near the termination of our experiments were uniformly low (i.e.,  $<0.05k_0C$ ). In the experiments of Bradford *et al.* [2002], on the other hand, the concentrations of retained colloid concentrations were considerably lower than the retention capacity of the porous media and hence high straining rates trapped most colloids near the tops of the columns.

[35] We find that a simple kinetics formulation is appropriate for simulating colloid straining within quartz sand and that the two parameters that govern this model vary in a systematic way with colloid and sand grain dimensions. These relationships between straining rates and easily measurable properties of the sand grains and colloids should contribute to quantitative descriptions of colloid transport in porous media. Despite this progress, our knowledge of factors that govern colloid straining is far from complete. Our experiments were conducted under ideal conditions and hence did not take into account many complexities associated with geologic environments and engineered systems. We used spherical colloids in our experiments, yet many, if not most, naturally occurring groundwater colloids have more complex shapes. Furthermore, groundwater suspensions, unlike our latex microsphere suspensions, are rarely characterized by uniform particle size. We used sieved, well-rounded quartz sand that was thoroughly cleaned to minimize physicochemical deposition, but natural aquifer materials are composed of mineral grains of varying size, shape, and roughness. These aquifer solids are typically coated with precipitates that promote physicochemical deposition, which, in turn, could enhance straining. Additional research that takes into account these complexities is requisite to continued advancement in our understanding of the movement of microbial pathogens and colloid-associated contaminants in geologic and engineered systems.

[36] **Acknowledgments.** This research was funded by National Science Foundation through grant EAR-0409174 and the Department of Energy through grant DE-FG07-02ER63492. We thank Alexis de Kerchove and Menachem Elimelech for their assistance with the colloid mobility measurements. We are also grateful to the Associate Editor, James Hunt, and three anonymous reviewers for their thorough and constructive comments that led to improvement of the manuscript.

## References

- Abudalo, R. A., Y. G. Bogatsu, J. N. Ryan, R. W. Harvey, D. W. Metge, and M. Elimelech (2005), Effect of ferric oxyhydroxide grain coatings on the transport of bacteriophage PRD1 and *Cryptosporidium parvum* oocysts in saturated porous media, *Environ. Sci. Technol.*, *39*, 6412–6419.
- Bhattacharjee, S., C. H. Ko, and M. Elimelech (1998), DLVO interaction between rough surfaces, *Langmuir*, *14*, 3365–3375.
- Bradford, S. A., and M. Bettahar (2005), Straining, attachment, and detachment of *Cryptosporidium* oocysts in saturated porous media, *J. Environ. Qual.*, *34*, 469–478.
- Bradford, S. A., and M. Bettahar (2006), Concentration dependent transport of colloids in saturated porous media, *J. Contam. Hydrol.*, *82*, 99–117.

- Bradford, S. A., S. R. Yates, M. Bettahar, and J. Simunek (2002), Physical factors affecting the transport and fate of colloids in saturated porous media, *Water Resour. Res.*, 38(12), 1327, doi:10.1029/2002WR001340.
- Bradford, S. A., J. Simunek, M. Bettahar, M. T. Van Genuchten, and S. R. Yates (2003), Modeling colloid attachment, straining, and exclusion in saturated porous media, *Environ. Sci. Technol.*, 37, 2242–2250.
- Bradford, S. A., M. Bettahar, J. Simunek, and M. T. Van Genuchten (2004), Straining and attachment of colloids in physically heterogeneous porous media, *Vadose Zone J.*, 3, 384–394.
- Bradford, S. A., J. Simunek, M. Bettahar, Y. F. Tadassa, M. T. Van Genuchten, and S. R. Yates (2005), Straining of colloids at textural interfaces, *Water Resour. Res.*, 41, W10404, doi:10.1029/2004WR003675.
- Elimelech, M. (1994), Effect of particle-size on the kinetics of particle deposition under attractive double-layer interactions, *J. Colloid Interface Sci.*, 164, 190–199.
- Elimelech, M., M. Nagai, C. H. Ko, and J. N. Ryan (2000), Relative insignificance of mineral grain zeta potential to colloid transport in geochemically heterogeneous porous media, *Environ. Sci. Technol.*, 34, 2143–2148.
- Foppen, J. W. A., A. Mporokoso, and J. F. Schijven (2005), Determining straining of *Escherichia coli* from breakthrough curves, *J. Contam. Hydrol.*, 76, 191–210.
- Gao, B., J. E. Saiers, and J. Ryan (2006), Pore-scale mechanisms of colloid deposition and mobilization during steady and transient flow through unsaturated granular media, *Water Resour. Res.*, 42, W01410, doi:10.1029/2005WR004233.
- Gregory, J. (1981), Approximate expressions for retarded van der Waals interaction, *J. Colloid Interface Sci.*, 83, 138–145.
- Happel, J. (1958), Viscous flow in multiparticle systems—Slow motion of fluids relative to beds of spherical particles, *AIChE J.*, 4, 197–201.
- Harvey, R. W., N. E. Kinner, D. Macdonald, D. W. Metge, and A. Bunn (1993), Role of physical heterogeneity in the interpretation of small-scale laboratory and field observations of bacteria, microbial-sized microsphere, and bromide transport through aquifer sediments, *Water Resour. Res.*, 29, 2713–2721.
- Havelaar, A. H., M. Vanolphen, and J. F. Schijven (1995), Removal and inactivation of viruses by drinking-water treatment processes under full-scale conditions, *Water Sci. Technol.*, 31, 55–62.
- Herzig, J. P., D. M. Leclerc, and P. Legoff (1970), Flow of suspensions through porous media—Application to deep filtration, *Ind. Eng. Chem.*, 62, 8–35.
- Hogg, R., T. W. Healy, and D. W. Fuerstenau (1966), Mutual coagulation of colloidal dispersions, *Trans. Faraday Soc.*, 62, 1638–1651.
- Keller, A. A., and S. Sirivithayapakorn (2004), Transport of colloids in unsaturated porous media: Explaining large-scale behavior based on pore-scale mechanisms, *Water Resour. Res.*, 40, W12403, doi:10.1029/2004WR003315.
- Kuznar, Z. A., and M. Elimelech (2004), Adhesion kinetics of viable *Cryptosporidium parvum* oocysts to quartz surfaces, *Environ. Sci. Technol.*, 38, 6839–6845.
- Li, X. Q., T. D. Scheibe, and W. P. Johnson (2004), Apparent decreases in colloid deposition rate coefficients with distance of transport under unfavorable deposition conditions: A general phenomenon, *Environ. Sci. Technol.*, 38, 5616–5625.
- Li, X. Q., C. L. Lin, J. D. Miller, and W. P. Johnson (2006a), Pore-scale observation of microsphere deposition at grain-to-grain contacts over assemblage-scale porous media domains using X-ray microtomography, *Environ. Sci. Technol.*, 40, 3762–3768.
- Li, X. Q., C. L. Lin, J. D. Miller, and W. P. Johnson (2006b), Role of grain-to-grain contacts on profiles of retained colloids in porous media in the presence of an energy barrier to deposition, *Environ. Sci. Technol.*, 40, 3769–3774.
- Press, W. H. (1989), *Numerical Recipes: The Art of Scientific Computing*, 702 pp., Cambridge Univ. Press, New York.
- Rajagopalan, R., and C. Tien (1976), Trajectory analysis of deep-bed filtration with sphere-in-cell porous-media model, *AIChE J.*, 22, 523–533.
- Redman, J. A., S. L. Walker, and M. Elimelech (2004), Bacterial adhesion and transport in porous media: Role of the secondary energy minimum, *Environ. Sci. Technol.*, 38, 1777–1785.
- Shellenberger, K., and B. E. Logan (2002), Effect of molecular scale roughness of glass beads on colloidal and bacterial deposition, *Environ. Sci. Technol.*, 36, 184–189.
- Sirivithayapakorn, S., and A. Keller (2003a), Transport of colloids in saturated porous media: A pore-scale observation of the size exclusion effect and colloid acceleration, *Water Resour. Res.*, 39(4), 1109, doi:10.1029/2002WR001583.
- Sirivithayapakorn, S., and A. Keller (2003b), Transport of colloids in unsaturated porous media: A pore-scale observation of processes during the dissolution of air-water interface, *Water Resour. Res.*, 39(12), 1346, doi:10.1029/2003WR002487.
- Song, L. F., P. R. Johnson, and M. Elimelech (1994), Kinetics of colloid deposition onto heterogeneously charged surfaces in porous media, *Environ. Sci. Technol.*, 28, 1164–1171.
- Tufenkji, N., and M. Elimelech (2004a), Correlation equation for predicting single-collector efficiency in physicochemical filtration in saturated porous media, *Environ. Sci. Technol.*, 38, 529–536.
- Tufenkji, N., and M. Elimelech (2004b), Deviation from the classical colloid filtration theory in the presence of repulsive DLVO interactions, *Langmuir*, 20, 10,818–10,828.
- Tufenkji, N., G. F. Miller, J. N. Ryan, R. W. Harvey, and M. Elimelech (2004), Transport of *Cryptosporidium* oocysts in porous media: Role of straining and physicochemical filtration, *Environ. Sci. Technol.*, 38, 5932–5938.
- Veerapaneni, S., and M. R. Wiesner (1996), Hydrodynamics of fractal aggregates with radially varying permeability, *J. Colloid Interface Sci.*, 177, 45–57.
- Veerapaneni, S., and M. R. Wiesner (1997), Deposit morphology and head loss development in porous media, *Environ. Sci. Technol.*, 31, 2738–2744.
- Yao, K. M., M. M. Habibian, and C. R. Omelia (1971), Water and waste water filtration—Concepts and applications, *Environ. Sci. Technol.*, 5, 1105–1112.

B. Gao, J. E. Saiers, and S. Xu, School of Forestry and Environmental Studies, Yale University, 205 Prospect Street, New Haven, CT 06511, USA. (james.saiers@yale.edu)